

## Tuning the Performance of Organic Spintronic Devices Using X-Ray Generated Traps

J. Rybicki,<sup>1</sup> R. Lin,<sup>1</sup> F. Wang,<sup>1</sup> M. Wohlgenannt,<sup>1,\*</sup> C. He,<sup>2</sup> T. Sanders,<sup>2</sup> and Y. Suzuki<sup>2,3,4</sup>

<sup>1</sup>*Department of Physics and Astronomy, Optical Science and Technology Center, University of Iowa, Iowa City, Iowa 52242, USA*

<sup>2</sup>*Department of Materials Science and Engineering, UC Berkeley, Berkeley, California 94720, USA*

<sup>3</sup>*Materials Sciences Division, Lawrence Berkeley National Laboratory, Berkeley, California 94720, USA*

<sup>4</sup>*Geballe Laboratory for Advanced Materials, Department of Applied Physics, Stanford University, Stanford, California 94305, USA*

(Received 20 April 2012; published 16 August 2012)

X rays produced during electron-beam deposition of metallic electrodes drastically change the performance of organic spintronic devices. The x rays generate traps with an activation energy of  $\approx 0.5$  eV in a commonly used organic. These traps lead to a dramatic decrease in spin-diffusion length in organic spin valves. In organic magnetoresistive (OMAR) devices, however, the traps strongly enhance magnetoresistance. OMAR is an intrinsic magnetotransport phenomenon and does not rely on spin injection. We discuss our observations in the framework of currently existing theories.

DOI: [10.1103/PhysRevLett.109.076603](https://doi.org/10.1103/PhysRevLett.109.076603)

PACS numbers: 72.25.Hg, 72.25.Dc, 72.80.Le, 75.47.Pq

In devices consisting of ferromagnetic electrodes and nonmagnetic spacer layers a significant difference in resistance can be observed between the parallel or antiparallel magnetization orientations. This effect is called giant magnetoresistance (GMR) or tunneling magnetoresistance (TMR) for a conducting or insulating spacer layer, respectively. Utilizing semiconductors as spacer-layers would be particularly attractive because of the possibility of implementing spintronic logic devices. However, spin injection into semiconductors continues to be challenging, in part, because of the conductivity mismatch problem [1]. The search for new material systems is therefore ongoing.

Recently, there has been increasing interest in using organic semiconductors for spintronics, motivated, in part, by their long spin relaxation times [2,3]. Both planar [4] and vertical [5] spin-valve devices using an organic semiconductor spacer layer and the ferromagnetic oxide  $\text{La}_{2/3}\text{Sr}_{1/3}\text{MnO}_3$  (LSMO) have been demonstrated.

In addition to the spin-valve effect, there exists another magnetoresistive effect that is particular to organic devices, the so-called organic magnetoresistive effect (OMAR). OMAR is a low-field, room-temperature magnetoresistive effect in organic semiconductor devices with nonmagnetic electrodes [6–9]. Even though the exact mechanism behind OMAR is still debated, there exists some agreement that the hydrogen hyperfine fields are involved, influencing spin-dependent reactions between paramagnetic species (polarons, triplet excitons) [10–12]. The hyperfine interaction can be viewed as the precession of the electronic spin about the local hyperfine field, which is a quasi-static magnetic field that varies randomly in direction from molecule to molecule [13]. Therefore hyperfine interaction is important also for spin valves: as the initially spin-polarized carriers diffuse through the device along different paths, the different local hyperfine-induced precessions they experience will lead to a dephasing and loss of spin polarization. Indeed, a successful theory of

spin diffusion in organic semiconductors has been formulated along these lines [14].

Although hyperfine interaction lies at the heart of both the current theories of OMAR and organic spin-valves, they depend on the hyperfine strength in a completely opposite way. Whereas hyperfine interaction causes the OMAR effect, and therefore the effect increases with increasing hyperfine strength, strong hyperfine fields cause spin-randomization and therefore reduce the observed spin-valve effect. Indeed, it has remained a significant mystery why then large OMAR and long spin-diffusion length are observed in organic devices using the same organic semiconductor, namely tris(8-hydroxyquinolino)aluminum ( $\text{Alq}_3$ ) [5,15]. Here we will show that the conditions for large OMAR and large GMR effect, respectively, are indeed complimentary to each other, and, in particular, that they depend on the trap concentration in opposite ways.

The motivation for the experiments that we report on here developed from an intriguing set of observations that we have made while working on organic spintronic devices over the years. We found that the performance of both OMAR and spin-valve devices very sensitively depends on whether the metallic layers are deposited by thermal evaporation or electron-beam evaporation. We will show that this behavior results from the generation of traps through the exposure of the organic layer to x-ray bremsstrahlung that is generated during the  $e$ -beam evaporation process. Our analysis of the role played by traps in organic spintronic devices will allow us to shed light on the physics of these devices, and indicate the possibility of using “trap engineering” to optimize the performance of organic magnetosensors.

The structure of our OMAR devices is largely identical to that of organic light emitting diodes (OLED). Our devices were fabricated on glass substrates, coated with 40 nm of indium tin oxide (ITO) and a  $\approx 100$  nm thick

layer of the conducting polymer Poly (3,4-ethylenedioxythiophene)-poly (styrene-sulfonate) (PEDOT). All subsequent manufacturing steps were carried out in a deposition chamber located inside a nitrogen glovebox. Next, the organic layer Alq<sub>3</sub> (70 to 100 nm) followed by the top electrode calcium (20 nm), and a capping layer of aluminum (40 nm) were deposited by thermal evaporation. Current-voltage ( $I$ - $V$ ), electroluminescence quantum efficiency,  $\eta_{EL}$  and magnetoconductivity (MC) experiments were performed on these devices. To study the effect of the electron beam's radiation, as it would have occurred if the metallic layers of the devices had been fabricated by  $e$ -beam evaporation, the devices were then returned into the deposition chamber, the electron beam (4.5 keV) was then turned on and directed onto a Au target for a time of up to 25 mins. We choose a beam current of  $\approx 40$  mA, a value typically used for Al evaporation, but insufficient for evaporation of the Au target. After this exposure, we again performed  $I$ - $V$ , electroluminescence quantum efficiency and magnetoconductivity experiments on these devices. Therefore, our procedure allows us to make accurate comparisons between pristine and radiation exposed devices. We emphasize that in our radiation treatment neither the  $e$ -beam nor any evaporated metal hits the OMAR device, rather the effects we report below must be due to a secondary radiation (which we will identify as bremsstrahlung).

We also completed an analogous study on spin valves, again comparing pristine and x-ray-exposed devices. Our spin-valve devices were fabricated on SrTiO<sub>3</sub> (STO) (001) substrates. On these substrates, a 1-mm wide, 100-nm thick LSMO film was fabricated by pulsed laser deposition through a shadow mask. The LSMO deposition was performed with a KrF excimer laser (248 nm) in 320 mTorr O<sub>2</sub> at 700 C with a laser fluence of 1–1.5 J/cm<sup>2</sup>, followed by postgrowth cooling in 300 Torr O<sub>2</sub>. The LSMO covered substrates were washed in several solvents using an ultrasonic cleaner and handled in a class 1000 clean-room. As the organic semiconductor spacer layer, the Alq<sub>3</sub> layer was fabricated by thermal evaporation in a vacuum of 10<sup>-6</sup> mbar at a rate of 0.1 nm/s. The Fe top electrodes were deposited by thermal evaporation. For comparison, a second group of otherwise identical devices was fabricated, this time using  $e$ -beam evaporation for the Fe top electrode. The device area for the OMAR and spin-valve devices was approximately 1 mm<sup>2</sup>.

Figure 1(a) shows  $I$ - $V$  measurements for Alq<sub>3</sub> OLED/OMAR devices irradiated for 0, 10, and 25 minutes at an  $e$ -beam current of 40 mA and an accelerating voltage of 4.5 kV. The onset voltage increases significantly with exposure time, the increase being approximately proportional to the exposure time. The larger electric fields that are required in the irradiated devices to drive a significant current are indicative of the presence of increased disorder within the irradiated Alq<sub>3</sub> film. Figure 1(b) shows that

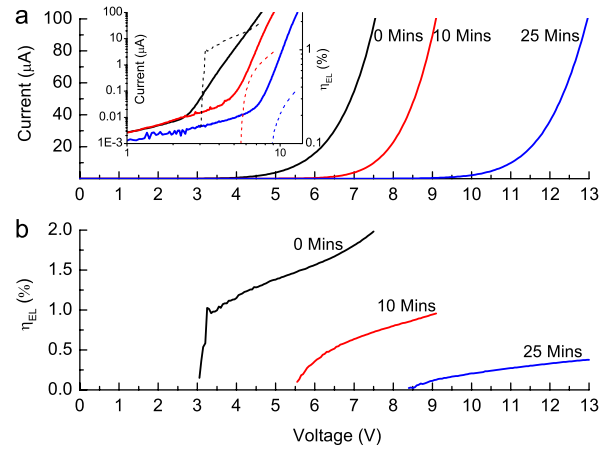


FIG. 1 (color online). The effect of x-ray irradiation on (a) current-voltage characteristics and (b) electroluminescence quantum efficiency, for PEDOT/Alq<sub>3</sub> (100 nm)/Ca devices with 25 minutes, 10 minutes, and zero minutes of exposure time. The inset shows the same current-voltage (solid) and electroluminescence-voltage (dotted) data on log-log scales.

irradiation also leads to a significant reduction in the electroluminescence quantum efficiency,  $\eta_{EL}$ .

It is widely known that bremsstrahlung is produced during  $e$ -beam evaporation: as the accelerated  $e$ -beam hits the metal target the electrons experience a sudden deceleration, and photons are emitted over a wide spectrum. We propose that it is the bremsstrahlung that leads to the irradiation effects we observe. Indeed, the destructive effect of bremsstrahlung on the organic layer was recently recognized and investigated [16].

In the Supplemental Material [17] we show that the x-ray irradiation produces traps in the organic semiconductor layer. We find that the concentration of traps is too low for them to be visible by standard spectroscopic techniques, such as infrared and Raman spectroscopies. This suggests that their concentration is at the sub-percent level. In the supplemental material we show that the thermally stimulated current (TSC) technique [18] allows the determination of the activation energy of these traps ( $\approx 0.5$  eV), and also provides a lower limit on the trap concentration of 10<sup>-7</sup> traps per Alq<sub>3</sub> molecule. However, we believe that the actual number of traps is much higher than this lower limit. Unfortunately, obtaining a quantitatively accurate value for the trap concentration has thus far eluded us (see the Supplemental Material [17] for further discussion).

An increase in onset voltage and a reduction in  $\eta_{EL}$ , similar to what we observed in Fig. 1, is also commonly observed in OLEDs if they are operated for extended periods due to a degradation mechanism [19,20]. This suggests that irradiation and temporal degradation share a common mechanism. It was shown, previously, that degradation effects in Alq<sub>3</sub> OLEDs are primarily caused by the hole-current [19], specifically, it was shown that Alq<sub>3</sub> cations [19,21] have the tendency to exhibit irreversible

reactions that produce traps and luminescence quenchers. Of course, x rays do not cause a hole-current, since the irradiation happens while the device is not operated. But just as in photoelectron spectroscopy (UPS and XPS) [22,23] the incident radiation will lead to the ejection of an electron from Alq<sub>3</sub> molecules, leaving behind a cation, which can then undergo irreversible trap-forming reactions.

We will now discuss the effect of traps on both OMAR and spin-valve devices, starting with the OMAR devices. Figure 2(a) shows magnetoconductance traces for the pristine as well as x-ray-exposed devices. The pristine device demonstrated only a small OMAR effect, with a maximum change in conductance of approximately 0.5%, whereas this value increased to 7.7% and 15.5% for the “10-minute” and “25-minute” devices, respectively (even longer exposure times lead to unstable devices). All OMAR traces shown are for the bias voltage that gives the largest magnetoconductance [see Figs. 2(b) and 2(c)]. Comparing Fig. 2(a) with the corresponding *I-V* and electroluminescence data in Figs. 1(a) and 1(b) we arrive at the, initially, somewhat surprising conclusion that the devices work best as OMAR devices, when they show the poorest performances as light emitting diodes and are the most resistive. However, our results are in agreement with recent reports [20,24] that demonstrated that the production of traps through “device conditioning” leads to an increase in magnetoconductance.

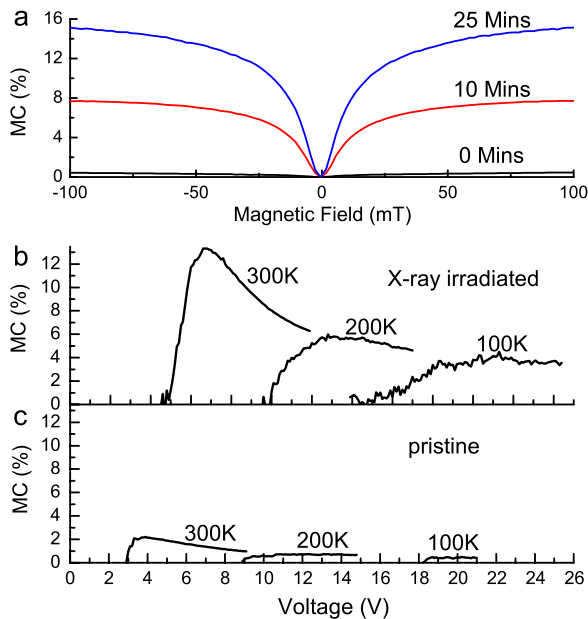


FIG. 2 (color online). (a) Magnetoconductance traces for the pristine and x-ray-exposed PEDOT/Alq<sub>3</sub> (70 nm)/Ca devices, respectively. (b) Dependence of the measured OMAR effect on the voltage for several different temperatures for x-ray irradiated (25 mins) device (c) Dependence of the measured OMAR effect on the voltage for several different temperatures for pristine device.

Next, we investigate the effect of traps on the spin-diffusion length. Figure 3(a) shows that the pristine and irradiated (20-minute) devices exhibit a spin-diffusion length at 12 K of  $\approx 40$  nm and  $\approx 7$  nm, respectively. This demonstrates that the spin-diffusion length in organic spin valves is very sensitive to the presence of traps. The remaining panels of Fig. 3 show additional data measured in the spin valves for completeness. The voltage dependence and temperature dependence we observe agree well with those observed by others, and we refer to the literature for a discussion of these dependencies [5]. Figure 4 shows measured *I-V* traces for the pristine (thick lines) and irradiated (thin lines) devices at 12 K with three different Alq<sub>3</sub> thicknesses, 5 nm (a), 20 nm (b), and 60 nm (c). The three panels show that the irradiated devices are dramatically more resistive and have *I-V* traces that are more non-linear. Further studies are required to uncover the nature of this dramatic change, but it is possible that it is related to bistability effects recently reported in organic spin-valves. Dediu and co-workers [25] suggested a mechanism for this bistability based on charge storage in deep traps. Our experiments may support this model, and provide a simple technique to quantitatively relate bistability and trap concentration in future work.

Let us now turn to the discussion of the experimental findings, starting with the reduction in spin-diffusion length. For the purpose of this discussion, we will compare this experimental observation with the expectations that arise from current theories of the spin-diffusion length in organic devices. To the best of our knowledge, two different

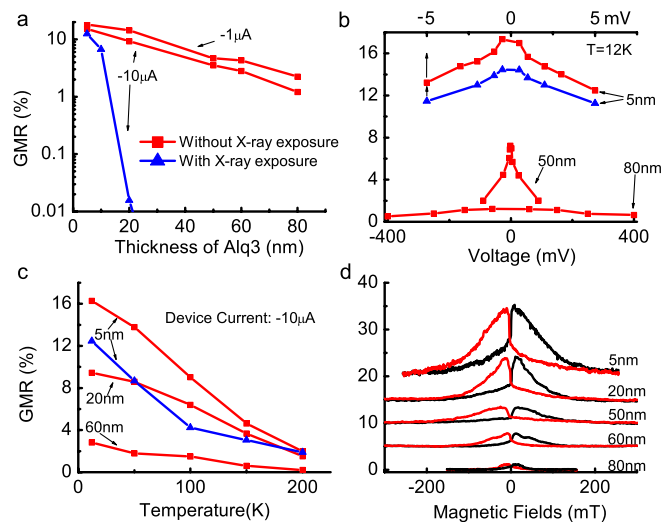


FIG. 3 (color online). (a) Thickness dependence of the magnitude of the observed spin-valve response at 12 K, both for a pristine device (scatter plots with square symbol) and an x-ray-exposed device (scatter plots with triangle symbol, 20 mins exposure time). From this data the spin-diffusion length can be extracted. (b) Voltage dependence of the observed spin-valve response at 12 K. (c) Temperature dependence of the magnitude of the observed spin-valve response. (d) Magnetoresistance traces at 12 K for the pristine device.

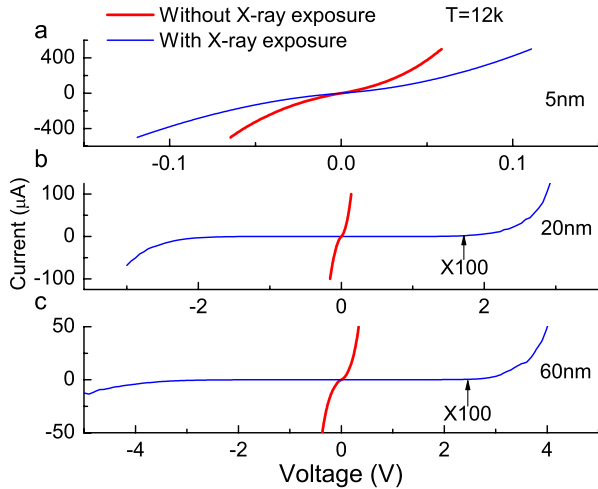


FIG. 4 (color online). Current-voltage (IV) characteristics for LSMO/Alq<sub>3</sub>/Co organic spin valves with three different organic layer thickness shown for both the pristine devices and x-ray-exposed devices.

such theories have been developed in detail so far. Chronologically, the first theory [14] is based on hyperfine interaction. As the carrier moves through the organic film, it will precess about the random local hyperfine fields, and carriers taking different paths through the film will dephase unpredictably. Bobbert *et al.* [14] have reported a detailed numerical Monte Carlo simulation of hyperfine-induced spin randomization as a function of various device and material parameters. These simulations showed that, in a certain limit, the spin-diffusion length,  $l_S$ , can be written as

$$l_S = \frac{r^2}{2} a, \quad (1)$$

where  $a$  is the intermolecular distance and  $r$  is the ratio of the spin-precession period to the average time the carrier spends on each site. We do not claim that we are in the limit where Eq. (1) holds strictly, but for a qualitative analysis this formula should be sufficient. It certainly captures the main idea of the hyperfine-limited spin-diffusion length, because the larger  $r$ , the faster the carrier moves and the less time there is for the hyperfine interaction to reorient the spin. Since traps slow down carrier motion, our experimental observation that the spin-diffusion length decreases is certainly in line with the hyperfine model.

The second model for the spin-diffusion length was proposed by Yu [26] and is based on spin-orbit coupling. Yu gave the following expression:

$$l_S = \frac{a}{4\gamma}, \quad (2)$$

where  $\gamma$  is a measure of the molecule-internal spin-orbit coupling strength. In this model the spin-diffusion length does not depend on mobility or the time the carrier spends on a site, but only on the number of hops the

carrier makes [26]. Therefore, this model appears to be incompatible with our experimental results.

Next, we explore the reason why OMAR is enhanced by traps and low mobility. The exact mechanism behind OMAR is currently not known with certainty. Several different models have been proposed [7,8,10,12,27–31]. However, all these models share a common basis: spin-dependent reactions that occur in paramagnetic pairs. The hyperfine interaction leads to a spin-mixing between singlet and triplet pairs. The potency of this mixing depends critically on the ratio  $r$ , which we introduced above. The potency is maximum if  $r$  is small (the so-called slow hopping regime) [12]. If  $r$  is large, however, then the local spin projection is not a good quantum number, and any spin-dependence in the pair reaction rates is weakened as the spin state is smeared out, so to speak, and hyperfine-induced spin-mixing becomes irrelevant. Therefore, it can readily be understood that the magnitude of OMAR increases as the hopping motion is slowed by the presence of traps. This mechanism applies equally to all mechanisms for OMAR which rely on hyperfine-induced singlet-triplet mixing. Specific to the bipolaron model [12] is another enhancement mechanism. The bipolaron mechanism is based on the formation of a doubly occupied molecular site. Such a doubly occupied site is however a high-energy state, since two carriers on the same site will strongly repel each other by the Coulomb force, and its formation is therefore suppressed by the corresponding Boltzmann factor. If, however, the already occupied site is a deep trap state, i.e., very low in energy, the negative energy of the trap can compensate the positive on-site repulsion, and bipolaron formation becomes much more probable.

In summary, we demonstrated that x rays produced during  $e$ -beam evaporation produce deep traps ( $\approx 0.5$  eV) that dramatically affect the performance of organic spintronic devices, including a strongly reduced spin diffusion length. It, therefore, appears that studies of the spin-diffusion length in devices fabricated by  $e$ -beam evaporation (e.g., [32,33]) may have to be carefully reevaluated. Somewhat unexpectedly, however, we found that traps lead to an enhanced OMAR response. Our finding suggests an interesting research program: careful control of the density and activation energy of the traps, as it could be achieved by thermal codeposition of two different organic semiconductors, may lead to highly sensitive organic magnetosensors.

This work was supported by ARO MURI under Grant No. W911NF-08-1-0317. J. R., R. L., and F. W. contributed equally to this work.

\*markus-wohlgenannt@uiowa.edu

- [1] G. Schmidt, D. Ferrand, L. W. Molenkamp, A. T. Filip, and B. J. van Wees, *Phys. Rev. B* **62**, R4790 (2000).
- [2] W. J. M. Naber, S. Faez, and W. G. van der Wiel, *J. Phys. D* **40**, R205 (2007).



- [3] V. A. Dediu, L. E. Hueso, I. Bergenti, and C. Taliani, *Nature Mater.* **8**, 707 (2009).
- [4] V. Dediu, M. Murgia, F. C. Maticcotta, C. Taliani, and S. Barbanera, *Solid State Commun.* **122**, 181 (2002).
- [5] Z. H. Xiong, D. Wu, Z. V. Vardeny, and J. Shi, *Nature (London)* **427**, 821 (2004).
- [6] T. L. Francis, O. Mermer, G. Veeraraghavan, and M. Wohlgenannt, *New J. Phys.* **6**, 185 (2004).
- [7] V. N. Prigodin, J. D. Bergeson, D. M. Lincoln, and A. J. Epstein, *Synth. Met.* **156**, 757 (2006).
- [8] B. Hu and Y. Wu, *Nature Mater.* **6**, 985 (2007).
- [9] F. L. Bloom, W. Wagemans, M. Kemerink, and B. Koopmans, *Phys. Rev. Lett.* **99**, 257201 (2007).
- [10] J. Kalinowski, M. Cocchi, D. Virgili, P. Di Marco, and V. Fattori, *Chem. Phys. Lett.* **380**, 710 (2003).
- [11] P. Desai, P. Shakya, T. Kreouzis, W. P. Gillin, N. A. Morley, and M. R. J. Gibbs, *Phys. Rev. B* **75**, 094423 (2007).
- [12] P. A. Bobbert, T. D. Nguyen, F. W. A. van Oost, B. Koopmans, and M. Wohlgenannt, *Phys. Rev. Lett.* **99**, 216801 (2007).
- [13] K. Schulten and P. G. Wolynes, *J. Chem. Phys.* **68**, 3292 (1978).
- [14] P. A. Bobbert, W. Wagemans, F. W. A. van Oost, B. Koopmans, and M. Wohlgenannt, *Phys. Rev. Lett.* **102**, 156604 (2009).
- [15] O. Mermer, G. Veeraraghavan, T. L. Francis, and M. Wohlgenannt, *Solid State Commun.* **134**, 631 (2005).
- [16] M. Yamada, M. Matsumura, and Y. Maeda, *Thin Solid Films* **519**, 6219 (2011).
- [17] See Supplemental Material at <http://link.aps.org/supplemental/10.1103/PhysRevLett.109.076603> for details of the thermally stimulated current technique to determine the properties of the x-ray generated traps; E. Shiles, T. Sasaki, M. Inokuti, and D. Y. Smith, *Phys. Rev. B* **22**, 1612 (1980); S. Karg, J. Steiger, and H. von Seggern, *Synth. Met.* **111–112**, 277 (2000); H. Bassler, *Phys. Status Solidi B* **175**, 15 (1993).
- [18] J. Steiger, R. Schmechel, and H. von Seggern, *Synth. Met.* **129**, 1 (2002).
- [19] H. Aziz, Z. D. Popovic, N. X. Hu, A. M. Hor, and G. Xu, *Science* **283**, 1900 (1999).
- [20] T. Schmidt, A. Buchschuster, M. Holm, S. Nowy, J. Weber, and W. Brutting, *Synth. Met.* **161**, 637 (2011).
- [21] F. Papadimitrakopoulos, X. M. Zhang, D. L. Thomsen, and K. A. Higginson, *Chem. Mater.* **8**, 1363 (1996).
- [22] R. Treusch, F. J. Himpsel, S. Kakar, L. J. Terminello, C. Heske, T. van Buuren, V. V. Dinh, H. W. Lee, K. Pakbaz, G. Fox, and I. Jimenez, *J. Appl. Phys.* **86**, 88 (1999).
- [23] A. DeMasi, L. F. J. Piper, Y. Zhang, I. Reid, S. Wang, K. E. Smith, J. E. Downes, N. Peltekis, C. McGuinness, and A. Matsuura, *J. Chem. Phys.* **129**, 224705 (2008).
- [24] U. Niedermeier, M. Vieth, R. Patzold, W. Sarfert, and H. von Seggern, *Appl. Phys. Lett.* **92**, 193309 (2008).
- [25] M. Prezioso, A. Riminucci, I. Bergenti, P. Graziosi, D. Brunel, and V. A. Dediu, *Adv. Mater.* **23**, 1371 (2011).
- [26] Z. G. Yu, *Phys. Rev. Lett.* **106**, 106602 (2011).
- [27] H. Odaka, Y. Okimoto, T. Yamada, H. Okamoto, M. Kawasaki, and Y. Tokura, *Appl. Phys. Lett.* **88**, 123501 (2006).
- [28] Y. Iwasaki, T. Osasa, M. Asahi, M. Matsumura, Y. Sakaguchi, and T. Suzuki, *Phys. Rev. B* **74**, 195209 (2006).
- [29] J. D. Bergeson, V. N. Prigodin, D. M. Lincoln, and A. J. Epstein, *Phys. Rev. Lett.* **100**, 067201 (2008).
- [30] E. L. Frankevich, A. A. Lymarev, I. Sokolik, F. E. Karasz, S. Blumstengel, R. H. Baughman, and H. H. Horhold, *Phys. Rev. B* **46**, 9320 (1992).
- [31] P. Desai, P. Shakya, T. Kreouzis, and W. P. Gillin, *Phys. Rev. B* **76**, 235202 (2007).
- [32] J. W. Yoo, H. W. Jang, V. N. Prigodin, C. Kao, C. B. Eom, and A. J. Epstein, *Phys. Rev. B* **80**, 205207 (2009).
- [33] R. Lin, F. Wang, J. Rybicki, M. Wohlgenannt, and K. A. Hutchinson, *Phys. Rev. B* **81**, 195214 (2010).